

Charged dust grain dynamics subject to solar wind, Poynting-Robertson drag, and the interplanetary magnetic field

Christoph Lhotka¹ and Philippe Bourdin and Yasuhito Narita

Space Research Institute, Austrian Academy of Sciences, Schmiedlstrasse 6, A-8042 Graz

`christoph.lhotka@oeaw.ac.at`

`philippe.bourdin@oeaw.ac.at`

`yasuhito.narita@oeaw.ac.at`

Received: date / Accepted: date

Received _____; accepted _____

Draft

¹Corresponding author.

ABSTRACT

We investigate the combined effect of solar wind, Poynting-Robertson drag, and the frozen-in interplanetary magnetic field on the motion of charged dust grains in our solar system. For this reason we derive a secular theory of motion by the means of averaging method and validate it with numerical simulations of the un-averaged equations of motions. The theory predicts that the secular motion of charged particles is mainly affected by the z-component of the solar magnetic axis, or the normal component of the interplanetary magnetic field. The normal component of the interplanetary magnetic field leads to an increase or decrease of semi-major axis depending on its functional form and sign of charge of the dust grain. It is generally accepted that the combined effects of solar wind and photon absorption and re-emission (Poynting-Robertson drag) lead to a decrease in semi-major axis on secular time scales. On the contrary, we demonstrate that the interplanetary magnetic field may counteract these drag forces under certain circumstances. We derive a simple relation between the parameters of the magnetic field, the physical properties of the dust grain as well as the shape and orientation of the orbital ellipse of the particle, which is a necessary conditions for the stabilization in semi-major axis.

Subject headings: Interplanetary magnetic field, solar wind drag, Poynting-Robertson drag, dust grains, celestial mechanics

1. Introduction

Micrometer-sized particles in the solar system originate from asteroid collisions and cometary activities, and can be found at various places in interplanetary space. The dynamics of uncharged micrometer-sized particles is influenced by different effects. First, the gravitational force attracts particles toward the Sun and the planets. Second, the solar radiation pressure pushes particles away from the Sun. Third, the combined solar wind and Poynting-Robertson effect brakes the particle motion due to a momentum transfer. These forces compete against one another such that some particles may fall onto the Sun, some leave the solar system, and some stay temporarily captured in the solar system (see, e.g. Mann et al. 2006, 2014).

Dust grains get charged by collecting and emitting charged particles. As a result the net charge and electrostatic potential of the dust grains change with time too. These changes finally end if a charge equilibrium has been reached. The main charging mechanisms in the solar system are as follows: i) impacts of electrons and ions directly transfer their charge to the grain; ii) photo-ejection of electrons by ultra-violet radiation of the Sun, as well as iii) recombination with free electrons from the dust grain environment. In the solar system the grains typically obtain a positive charge due to the dominance of ii) that corresponds to values of the electric potential of the order of 1-10 Volts, i.e. 5 Volts for grains around 1 micron in diameter.

Here, we conduct an analytical and numerical study on the impact of the normal magnetic field component, with respect to the equator of the Sun, to the orbital dynamics of micrometer-sized particles in the interplanetary magnetic field. Usually, the influence of the normal component of the interplanetary field on the micrometer-sized particle dynamics

is neglected. Naively speaking, one may anticipate that the magnetic field imposes a change in particle orbits (e.g., the inclination, the eccentricity, or the semi-major axis) through gyro-motion around the magnetic field, the adiabatic change against the inhomogeneous magnetic field, and drift motions in a gravitational field. We start with the equation of motion for the electrically charged, micrometer-sized particles and investigate the time evolution of the orbits, as well as an equilibrium state imposed by the magnetic field, both incorporating an axi-symmetric spiral shape of the planar interplanetary magnetic field (Parker 1958; Weber & Davis 1967). We find that the normal component of the magnetic field with respect to the equatorial plane of the Sun, i.e. the orbital plane of the particle plays a crucial role. The likely magnitude of the normal magnetic field component can be estimated on the basis of the fast pole to pole transit of the Ulysses spacecraft at solar minimum activity. We make use of the analysis in Forsyth et al. (1996, 2002) of the spacecraft data to find representative values of the magnetic field components. A 3-dimensional model of the heliospheric magnetic field has also been used in Zurbuchen et al. (1997), where the authors find that the normal component scales with the inverse distance between the particle and the magnetic source.

The secular orbital evolution of dust grains due to solar wind and Poynting-Robertson drag alone has been investigated, e.g. in Klačka (2013). An important contribution to the research of motion of charged dust particles in interplanetary fields can be found in Morfill & Grün (1979a,b). Here, the authors provide a detailed analysis of various systematic effects caused by electromagnetic forces on the orbital parameters of charged dust grains, i.e. they show that small stochastic variations induced by these forces are unimportant for particles of sufficient mass. The interplay between drag and Lorentz forces has been investigated in Mukai & Giese (1984), where the authors find that the Lorentz force introduces a significant effect on the orbital inclination i , while the effect on the variation

in semi-major axis a is negligible. Stochastic diffusion of interplanetary dust grains orbiting under Poynting-Robertson drag force and within the interplanetary field has been discussed in Wallis & Hassan (1985). In Fahr et al. (1995) the authors find that particle distributions depend on inclination and distance from the Sun in the case of asymmetric solar winds. The drift in inclination i due to electromagnetic force has been studied in detail in Fahr et al. (1981). This work predicts that dust can be expected to be concentrated close to the magnetic equator. The dynamics of dust in the vicinity of the Sun has been treated in Krivov et al. (1998a), where the authors find that the orientation of the orbital planes of the particles is dictated by electromagnetic forces. Typical dynamical evolution of charged dust particles has also been treated in Krivov et al. (1998b). The authors find that the radial motion of particles are relatively insensitive to the electromagnetic force, while orbital planes are affected depending on the size and chemical composition. The interactions of dust grains with coronal mass ejections and solar cycle variations are analyzed in Ragot & Kahler (2003). Numerical simulations of particle orbits subject to Lorentz force, solar wind, and Poynting-Robertson drag can be found in Kocifaj & Klačka (2004); Kocifaj et al. (2006). In the latter, the authors mainly focus on the temperature-dependent dielectric functions of carbonaceous or silicate particles, but also provide a numerical study of the long-term dynamics of micrometer-sized particles with changing optical properties. In Mann et al. (2007) the authors show that nanometer-sized particles can stay in bound orbits and, aside from the Lorentz force, the plasma and the photon Poynting-Robertson effect determine their spatial distribution.

Closest related with our study is Consolmagno (1979), where the mean square change in the orbital elements due to electromagnetic interactions is compared with the net Poynting-Robertson effect. The author states: *"Lorentz scattering can maintain significant numbers of micron and submicron particles against loss from the solar system due to Poynting-Robertson drag."* While, the author further wrote *"...there is no obvious way to*

calculate the magnitude of these secular changes...” (of the orbital elements), the author already estimated that *“...there may well be secular changes in the orbital elements due to Lorentz force.”*

With our study we would like to quantify these statements. We describe the secular evolution of the orbital elements due to Lorentz force by means of Equations (13), (14) in Section 2.3., and we provide a charge over mass ratio to balance the Lorentz force with solar wind and Poynting-Robertson drag force by means of Equation (22) in Section 2.5.

2. The dynamical model

We investigate the dynamics of micro-meter sized, spherical particles of radius R , density ρ , and mass m orbiting in our solar system.

2.1. Set-up of notation and Cartesian framework

Let $\mathbf{e}_x = (1, 0, 0)$, $\mathbf{e}_y = (0, 1, 0)$, $\mathbf{e}_z = (0, 0, 1)$ be Cartesian unit vectors in a heliocentric coordinate system. We denote by \mathbf{r} , \mathbf{v} the Cartesian position and velocity of the dust grain with scalar distance $r = \|\mathbf{r}\|$ from the Sun. Moreover, $\mu \equiv GM$ is the heliocentric gravitational constant, S is the solar energy flux at distance r , A is the cross-sectional area of the grain, Q is the spectrally averaged dimensionless efficiency factor of the radiation pressure, and c is the speed of light. We introduce the ratio of solar radiation pressure over solar gravitational attraction:

$$\beta = \frac{SAQ}{c} / \frac{GMm}{r^2} . \quad (1)$$

Since $S \propto 1/r^2$ we notice that β is a dimensionless parameter without radial dependence. Let \mathbf{u}_{sw} be the velocity vector of the solar wind with magnitude u_{sw} , and η be the dimensionless solar wind drag efficiency factor (the ratio of solar wind over Poynting-Robertson drag). Furthermore, \mathbf{r}_1 is the Cartesian position of an additional planet of mass m_1 in the heliocentric reference frame. Moreover, we denote by B_0 the magnetic field strength at the reference distance r_0 of the magnetic field \mathbf{B} that originates from the Sun. The equation of motion of the particle of charge $q = 4\pi\epsilon_0 UR$ is given by:

$$\begin{aligned} \frac{d\mathbf{v}}{dt} = & -\frac{(1-\beta)\mu}{r^2}\mathbf{e}_R - \frac{\beta\mu}{r^2}\left(1 + \frac{\eta}{Q}\right)\left(\frac{(\mathbf{v} \cdot \mathbf{e}_R)\mathbf{e}_R + \mathbf{v}}{c}\right) \\ & - Gm_1\left(\frac{\mathbf{r}_1}{r_1^3} + \frac{\mathbf{r} - \mathbf{r}_1}{\|\mathbf{r} - \mathbf{r}_1\|^3}\right) + \frac{q}{m}(\mathbf{v} - \mathbf{u}_{sw}) \times \mathbf{B} , \end{aligned} \quad (2)$$

where ϵ_0 is the permittivity of vacuum, and U denotes the particle's surface potential. Let $\boldsymbol{\omega} = (\omega_1, \omega_2, \omega_3)$ be the direction of the magnetic axis of the Sun given in the heliocentric frame of reference. We denote by $\mathbf{e}_R = \mathbf{r}/r$, $\mathbf{e}_T = \boldsymbol{\omega} \times \mathbf{e}_R$, and $\mathbf{e}_N = \boldsymbol{\omega}$ the radial, tangential, and normal unit vectors in a body fixed reference frame attached to the Sun. The magnetic field can be decomposed in terms of the radial B_R , tangential B_T , and normal component B_N as follows:

$$\mathbf{B} = B_R\mathbf{e}_R + B_T\mathbf{e}_T + B_N\mathbf{e}_N . \quad (3)$$

In this framework, a radially expanding and uniform solar wind is given by:

$$\mathbf{u}_{sw} = u_{sw}\mathbf{e}_R . \quad (4)$$

Equation (2) reduces for $\beta = 0$, $m_1 = 0$, and $q/m = 0$ to the integrable two-body problem. For $\beta \neq 0$ the first term corresponds to the solar radiation pressure of the

two-body problem with reduced central mass $(1 - \beta)$. The second term is the sum of the drag terms due to solar wind friction and the Poynting-Robertson effect. The third term is the gravitational perturbation due to the additional planet. The last term is the acceleration that a charged grain experiences due to the presence of a "frozen-in" magnetic field, and in absence of a background electric current resistivity ($\mathbf{E} = -\mathbf{u}_{sw} \times \mathbf{B}$). "Frozen-in" refers to the magnetic and thermal plasma pressure, where in the solar wind the magnetic field is frozen-in to the plasma bulk motion.

2.2. Gauss' form of the equations of motions

We denote the orbital elements of the particle by the semi-major axis a , the eccentricity e , the inclination i , the argument of perihelion ω , the longitude of the ascending node Ω , true anomaly f , and the mean anomaly M . The norm of the orbital angular momentum is then given by $h = \sqrt{1 - e^2} \sqrt{\mu a}$. Kepler's 3rd law is $\mu = n^2 a^3$, where n is the mean motion of the dust grain. In this setting, Gauss' form of perturbed equations of motion are given by (c.f. Fitzpatrick 1970):

$$\begin{aligned}
 \frac{da}{dt} &= \frac{2ah}{\mu(1 - e^2)} [e \sin f F_R + (1 + e \cos f) F_T] , \\
 \frac{de}{dt} &= \frac{h}{\mu} [\sin f F_R + (\cos f + \cos E) F_T] , \\
 \frac{di}{dt} &= \frac{\cos(\omega + f) r}{h} F_N , \\
 \frac{d\omega}{dt} &= -\frac{h}{\mu} \frac{1}{e} \left[\cos f F_R - \left(\frac{2 + e \cos f}{1 + e \cos f} \right) \sin f F_T \right] - \frac{\cos i \sin(\omega + f) r F_N}{h \sin i} , \\
 \frac{d\Omega}{dt} &= \frac{\sin(\omega + f) r}{h \sin i} F_N , \\
 \frac{dM}{dt} &= n + \frac{h \sqrt{1 - e^2}}{\mu e} \left[\left(\cos f - \frac{2e}{1 - e^2} \frac{r}{a} \right) F_R - \left(1 + \frac{1}{1 - e^2} \frac{r}{a} \right) \sin f F_T \right] .
 \end{aligned} \tag{5}$$

Here, F_R , F_T , F_N are the radial, tangential, and normal components of the perturbing force $F = F_R \mathbf{e}'_R + F_T \mathbf{e}'_T + F_N \mathbf{e}'_N$ given in the orbital frame of the particle: $\mathbf{e}'_R = (\cos f, \sin f, 0)$, $\mathbf{e}'_T = (-\sin f, \cos f, 0)$, and $\mathbf{e}'_N = \mathbf{e}'_R \times \mathbf{e}'_T$. The relation between orbital and heliocentric reference frame is provided by the rotation matrix¹

$$\mathfrak{R} = \mathfrak{R}_3(\Omega) \cdot \mathfrak{R}_1(i) \cdot \mathfrak{R}_3(\omega) . \quad (6)$$

For a generic force given in the heliocentric reference frame in terms of $\mathbf{F} = F_x \mathbf{e}_x + F_y \mathbf{e}_y + F_z \mathbf{e}_z$ the following relations hold true:

$$F_R = (F_x, F_y, F_z) \cdot \mathfrak{R} \cdot \mathbf{e}'_R , \quad F_T = (F_x, F_y, F_z) \cdot \mathfrak{R} \cdot \mathbf{e}'_T , \quad F_N = (F_x, F_y, F_z) \cdot \mathfrak{R} \cdot \mathbf{e}'_N . \quad (7)$$

Thus, if we identify \mathbf{F} with the perturbing parts of the Kepler problem in Equation (2) (i.e. without the term that defines the unperturbed two body problem) then it is true that Equations (5) are equivalent with the equations of motion defined by Equation (2). Using well known formulae for Taylor series expansions in the two-body problem (c.f. Dvorak & Lhotka 2013) the right hand sides of Equation (5) can be written in terms of orbital elements of the dust particle and the perturbing planet, only. For $\beta = 0$, $m_1 = 0$, and $q/m = 0$ the system of Equations (5) reduces to the single integrable equation of motion $dM/dt = n$.

¹The rotation matrices are defined as follows:

$$\mathfrak{R}_1(\varphi) = \begin{pmatrix} 1 & 0 & 0 \\ 0 & \cos \varphi & -\sin \varphi \\ 0 & \sin \varphi & \cos \varphi \end{pmatrix} , \quad \mathfrak{R}_3(\varphi) = \begin{pmatrix} \cos \varphi & -\sin \varphi & 0 \\ \sin \varphi & \cos \varphi & 0 \\ 0 & 0 & 1 \end{pmatrix} .$$

2.3. The magnetized two body problem

Lhotka & Celletti (2015) have treated the influence of solar radiation pressure, solar wind, and Poynting-Robertson drag force. In this Section, we are mainly interested in additional effects of the Lorentz-force. Let the components of a generic interplanetary magnetic field in Equation (3) be the product of constant, radially dependent, and time dependent terms:

$$B_R = B_{R0} \left(\frac{r_0}{r} \right)^2 b_R(t) , \quad B_T = B_{T0} \left(\frac{r_0}{r} \right) b_T(t) , \quad B_N = B_{N0} \left(\frac{r_0}{r} \right)^\kappa b_N(t) . \quad (8)$$

Here, B_{R0} , B_{T0} , B_{N0} are the components of the average magnetic field background strength at reference distance r_0 , and b_R , b_T , b_N are periodic functions in time, that are introduced to mimic the solar cycle. The radial dependencies $1/r^2$ in B_R and $1/r$ in B_T resemble those of the classical Parker spiral (c.f. Parker 1958; Grün et al. 1994; Meyer-Vernet 2007). Assuming a radial magnetic field of the source and a purely radial expansion of the solar wind it is possible to set $B_N = 0$ and we recover the time dependent Parker spiral (c.f. Kocifaj et al. 2006) with:

$$b_R(t) = \cos(2\pi t/T + \varphi_0) , \quad b_T(t) = \cos(\vartheta) \cos(2\pi t/T + \varphi_0) , \quad (9)$$

where φ_0 is the magnetic phase angle and ϑ is the altitude from the solar equatorial plane. T is the period of the solar magnetic cycle equal to about 22 years. Here, we now add the effect of a non-zero normal component of the magnetic field $B_N \neq 0$ on the particle dynamics. According to Zurbuchen et al. (1997) the normal component scales with

$1/r$, i.e. $\kappa = 1$ in Equation (8). To understand the role of the exponent in $1/r$ on the secular motions we also include $\kappa = 2, 3$ in our study. We notice that B_N is not necessarily consistent with $\nabla \cdot \mathbf{B} = 0$ unless we add small extra dependencies that could lead to a consistent value for B_N . However, we argue that these additional contributions are small on average and do not alter our results on secular time scales, i.e. on the basis of a mean interplanetary magnetic field. Let $B'_R = B_{R0} \cdot b_R(t)$, $B'_T = B_{T0} \cdot b_T(t)$, and $B'_N = B_{N0} \cdot b_N(t)$. If we plug in Equation (8) in Equation (3), the right hand sides of the first three of Equations (5) become of the form:

$$\begin{aligned}
 \frac{da}{dt} &= \frac{q}{m} \frac{u_{sw}}{n} \left(\left[\frac{r_0}{a} \right] B'_T [1] + \left[\frac{r_0}{a} \right]^\kappa \left(c_{\mathbf{0}}^{(2,3)} \omega_3 + [2] \right) B'_N \right) \\
 \frac{de}{dt} &= \frac{q}{m} \left(\left\{ \frac{u_{sw}}{n} \left[\frac{r_0}{a} \right]^2 [3] + \left[\frac{r_0}{a} \right] [4] \right\} B'_T \right. \\
 &\quad \left. + \left\{ \frac{u_{sw}}{na} \left[\frac{r_0}{a} \right]^\kappa \left(c_{\mathbf{0}}^{(5,3)} \omega_3 + [5] \right) + \left[\frac{r_0}{a} \right]^\kappa [6] \right\} B'_N \right) \\
 \frac{di}{dt} &= \frac{q}{m} \left(\left[\frac{r_0}{a} \right]^2 [A] B'_R + \left\{ \frac{u_{sw}}{n} \left[\frac{r_0}{a} \right]^2 [7] + \left[\frac{r_0}{a} \right] [8] \right\} B'_T \right. \\
 &\quad \left. + \left\{ \frac{u_{sw}}{na} \left[\frac{r_0}{a} \right]^\kappa \left(c_{\mathbf{0}}^{(9,3)} \omega_3 + [9] \right) + \left[\frac{r_0}{a} \right]^\kappa [10] \right\} B'_N \right) .
 \end{aligned} \tag{10}$$

Here, each term $[\#]$ in Equation (10) takes the structural form:

$$[\#] = \sum_{\ell=1,2,3} \omega_\ell \left\{ \sum_{\mathbf{k} \in \mathbb{Z}^3} \frac{c_{\mathbf{k}}^{(\#, \ell)}}{s_{\mathbf{k}}^{(\#, \ell)}} (e, i) \frac{\cos}{\sin} (k_1 M + k_2 \omega + k_3 \Omega) \right\} , \tag{11}$$

while the term $[A]$ proportional to the only radial contribution B_R in Equation (10) becomes:

$$[A] = \sum_{\mathbf{k} \in \mathbb{Z}^3} \frac{c_{\mathbf{k}}^{(A)}}{s_{\mathbf{k}}^{(A)}} (e, i) \frac{\cos}{\sin} (k_1 M + k_2 \omega + k_3 \Omega) . \tag{12}$$

Second order Taylor series expansions of the coefficients $c_{\mathbf{k}}$, $s_{\mathbf{k}}$, that are valid in small eccentricity e , are provided in Appendix A. We notice, that the radial contribution B_R appears only in the equation for di/dt in Equation (10). Moreover, the radial component of the magnetic field is independent of the choice of $\boldsymbol{\omega}$, as expected. In addition, while for a vanishing solar wind speed $da/dt = 0$, the components de/dt , di/dt do not vanish.

The terms $[\#]$ and $[A]$ are periodic functions of zero average and wave number \mathbf{k} . Using averaging theory, we may neglect these terms, and investigate the long term dynamics by setting $[\#] = 0$, $[A] = 0$ in Equation (10). We obtain the secular system:

$$\begin{aligned}\frac{da}{dt} &= \omega_3 B'_N \left(\frac{r_0}{a}\right)^\kappa \frac{q}{m} \frac{u_{sw}}{n} g_{\kappa,a}(e) \cos i, \\ \frac{de}{dt} &= \omega_3 B'_N \left(\frac{r_0}{a}\right)^\kappa \frac{q}{m} \frac{u_{sw}}{na} g_{\kappa,e}(e) \cos i, \\ \frac{di}{dt} &= \omega_3 B'_N \left(\frac{r_0}{a}\right)^\kappa \frac{q}{m} \frac{u_{sw}}{na} g_{\kappa,i}(e) \sin i,\end{aligned}\tag{13}$$

where $g_{\kappa,a}$, $g_{\kappa,e}$, $g_{\kappa,i}$ are functions of eccentricity e , originating from the coefficients $c_{\mathbf{0}}^{(2,3)}$, $c_{\mathbf{0}}^{(5,3)}$, and $c_{\mathbf{0}}^{(9,3)}$, respectively. A Taylor series expansion of order 4 in small eccentricity e can be found in Appendix A.

We immediately recognize, that only the normal component B_N of Equation (8) can lead to a secular motion, i.e. drift in the semi-major axis, the eccentricity, and inclination on secular time scales. An order of magnitude comparison of the right hand sides of Equations (13) shows that $de/da = 1/a$, and $di/dt \rightarrow 0$ for small inclination $i \rightarrow 0$.

What about the qualitative behaviour of the angle-like Kepler elements ω , Ω , M ? It turns out, that the right hand side of $d\omega/dt$, $d\Omega/dt$ in Equation (5) are affected in a similar

way as di/dt , i.e. by radial, tangential, and normal components of the magnetic field, while the right hand side of dM/dt is not affected by the radial component B_R (comparable to the case da/dt described above). The same approach as for the action-like Kepler elements a, e, i , leads us to a secular system of the angle-like variables ω, Ω and M :

$$\begin{aligned}\frac{d\omega}{dt} &= \omega_3 B'_N \left(\frac{r_0}{a}\right)^\kappa \frac{q}{m} g_{\kappa,\omega}(e) \cos i , \\ \frac{d\Omega}{dt} &= \omega_3 B'_N \left(\frac{r_0}{a}\right)^\kappa \frac{q}{m} g_{\kappa,\Omega}(e) , \\ \frac{dM}{dt} &= n + \omega_3 B'_N \left(\frac{r_0}{a}\right)^\kappa \frac{q}{m} g_{\kappa,M}(e) \cos i .\end{aligned}\tag{14}$$

Here, $g_{\kappa,\omega}$, $g_{\kappa,\Omega}$, and $g_{\kappa,M}$ denote the eccentricity functions of the angle-like variables, provided also, in Appendix A. We notice, that the secular components of the angle-like variables are stemming from the terms independent of the solar wind velocity – opposite to the secular terms of the action-like variables in Equation (13).

We now directly compare a numerical integration of the original set of Equations (2) for $\beta = 0$, $m_1 = 0$ with the secular system defined by Equations (13), (14), using $\varphi = 0$, $\vartheta = 0$, $\kappa = 2$, and $T = 22\text{yrs}$. We choose for the normal magnetic field component:

$$b_N(t) = 1 + \cos(2\pi t/T) .\tag{15}$$

The choice is motivated to allow B_N to be of non-zero average, with the additional property to be periodic in the magnetic solar cycle. The constant in Equation (15) is used to demonstrate its effect on the secular evolution of the orbital elements, i.e. drift. The periodic term ensures that the normal component varies with the same period as the remaining components of the magnetic field, i.e. B_R, B_T in Equation (9). While the

existence of a non-zero normal component of the magnetic field has already been observed, e.g. in Zurbuchen et al. (1997) one may question the validity of Equation (15). Does a persistent and significant non-zero value for B_N exist? Indeed there are indications that a north-south asymmetry in the solar magnetic field causes a persistent average cone-shaped asymmetry of the heliospheric magnetic field, which is called the "bashful ballerina" (Hiltula & Mursula 2006; Mursula & Virtanen 2012). We estimate the magnitude of B_N from measurements of the Ulysses spacecraft during its polar orbit around the Sun. We make use of the analysis of the data provided in Forsyth et al. (2002), where the authors investigate deviations from the standard Parker model in terms of the meridional angle δ_B . In this setting the magnitude of B_N may be obtained from $\sin \delta_B = B_N/|\mathbf{B}|$ (see appendix) for given δ_B and $|\mathbf{B}|$.

In Figure 1 we show the comparison between the complete and simplified system. We find that Equations (13), (14) well describe the secular dynamics of the complete system defined by Equation (2) on secular time scales. The orbit corresponds to the motion of charged particles with radius $R = 1\mu m$, density $\rho = 2g/cm^3$, with the surface electric potential of $U = +5V$. For the simulation we use $B_{R0} = B_{T0} = 3 \times 10^{-9} T$ and $B_{N0} = 0.5 \times 10^{-9} T$ at $r_0 = 1au$. We choose the slow solar wind speed $u_{sw} = 400km/s$, and set the magnetic axis to $\omega_3 = \cos(7.25^\circ)$. Initial conditions are $a(0) = 1$, $e(0) = 0.1$, $i(0) = 20^\circ$, $\omega(0) = \Omega(0) = M(0) = 180^\circ$, respectively.

2.4. Near Hamiltonian form

Let $L = \sqrt{\mu a}$, $G = L\sqrt{1 - e^2}$, $H = G \cos i$, $l = M$, $g = \omega$, and $h = \Omega$ be the proper action-angle variables to our problem (usually referred to as Delaunay variables). The derivatives of these variables with respect to time are:

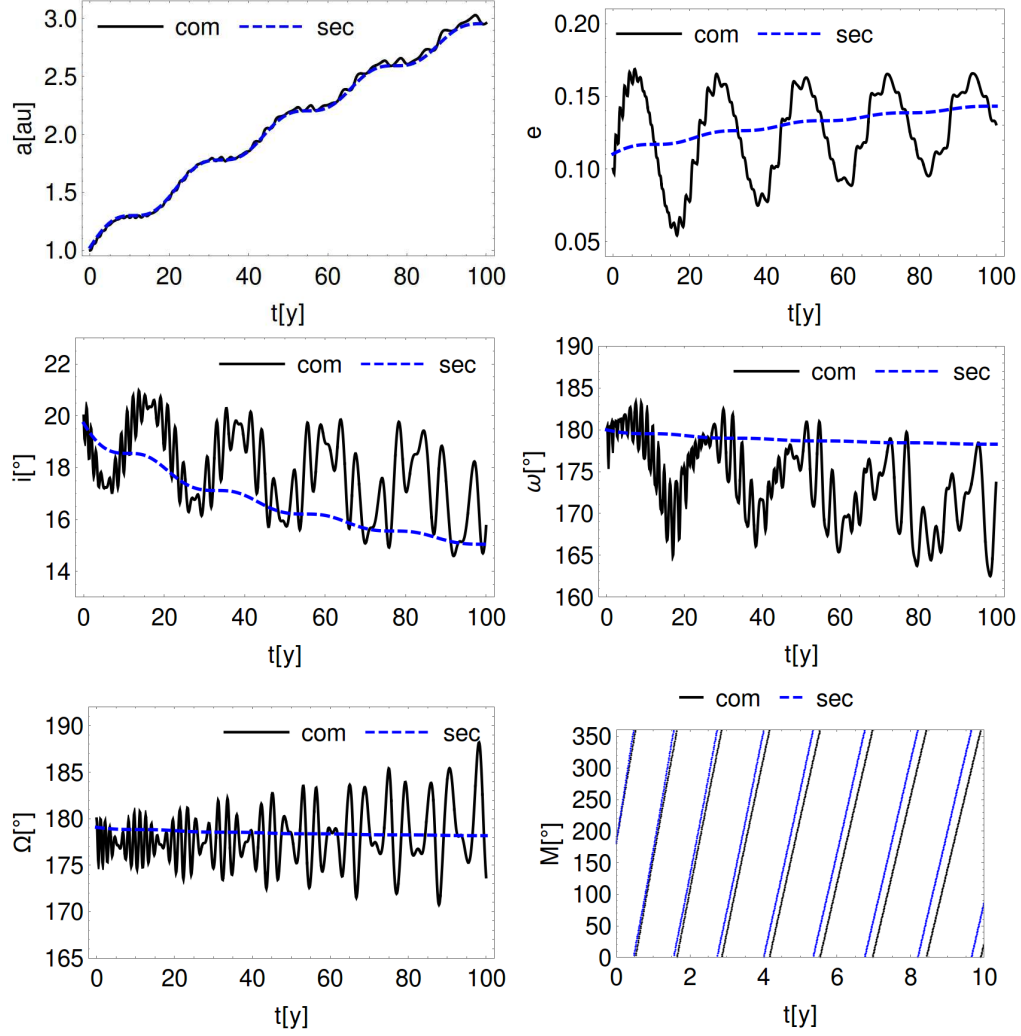


Fig. 1.— Comparison of Equation (2) ('com'plete, black) and Equations (13), (14) ('sec'ular, dashed blue) dynamics based on Equation (15). From upper left to lower right: semi-major axis a , eccentricity e , inclination i , argument of perihelion ω , longitude of ascending node Ω , mean anomaly M .

$$\begin{aligned}
\frac{dL}{dt} &= \frac{\mu}{2L} \frac{da}{dt}, \quad \frac{dl}{dt} = \frac{dM}{dt}, \\
\frac{dG}{dt} &= \frac{\mu G}{2L^2} \frac{da}{dt} - \frac{L\sqrt{L^2 - G^2}}{G} \frac{de}{dt}, \quad \frac{dg}{dt} = \frac{d\omega}{dt}, \\
\frac{dH}{dt} &= -\frac{\mu H}{2L^2} \frac{da}{dt} + \frac{HL\sqrt{L^2 - G^2}}{G} \frac{de}{dt} - \sqrt{G^2 - H^2} \frac{di}{dt}, \quad \frac{dh}{dt} = \frac{d\Omega}{dt}.
\end{aligned} \tag{16}$$

We remark that, due to the velocity dependent terms in Equation (2), the system of Equations (16) can not be derived from a potential for the velocity dependent terms that are associated to solar wind and Poynting-Robertson drag, as well as the magnetic field. However, Equations (16) are still of the special form:

$$\begin{aligned}
\frac{dL}{dt} &= -\frac{d\mathfrak{H}}{dl} + \mathfrak{f}_L, \quad \frac{dG}{dt} = -\frac{d\mathfrak{H}}{dg} + \mathfrak{f}_G, \quad \frac{dH}{dt} = -\frac{d\mathfrak{H}}{dh} + \mathfrak{f}_H, \\
\frac{dl}{dt} &= \frac{d\mathfrak{H}}{dL} + \mathfrak{f}_l, \quad \frac{dg}{dt} = \frac{d\mathfrak{H}}{dG} + \mathfrak{f}_g, \quad \frac{dh}{dt} = \frac{d\mathfrak{H}}{dH} + \mathfrak{f}_h,
\end{aligned} \tag{17}$$

where \mathfrak{H} denotes the Hamiltonian part, and $\mathfrak{f}_L, \mathfrak{f}_G, \mathfrak{f}_H$ as well as $\mathfrak{f}_l, \mathfrak{f}_g, \mathfrak{f}_h$ denote the non-conservative parts of Equation (2), only. For $\beta = 0, q/m = 0$ the underlying dynamical system is integrable, thus Equation (17) – and therefore also Equation (2) – is a nearly conservative, weakly dissipative dynamical system (see Celletti & Lhotka 2012; Lhotka & Celletti 2013). The total time derivative of the Hamiltonian is given by:

$$\Phi = \frac{\partial \mathfrak{H}}{\partial L} \frac{dL}{dt} + \frac{\partial \mathfrak{H}}{\partial G} \frac{dG}{dt} + \frac{\partial \mathfrak{H}}{\partial H} \frac{dH}{dt} + \frac{\partial \mathfrak{H}}{\partial l} \frac{dl}{dt} + \frac{\partial \mathfrak{H}}{\partial g} \frac{dg}{dt} + \frac{\partial \mathfrak{H}}{\partial h} \frac{dh}{dt} + \frac{d\mathfrak{H}}{dt}. \tag{18}$$

Taking for \mathfrak{H} only the terms in Equation (2) that correspond to the two-body problem, but taking for the time derivatives of the Delaunay variables, Equation (17) we find:

$$\Phi = \frac{\mu^2}{2a^2} \frac{da}{dt}, \tag{19}$$

with da/dt taken from Equation (13).

2.5. Balance of forces

We are interested in the long-term evolution of charged particles subject to Lorentz force, solar radiation pressure, solar wind, and Poynting-Robertson drag forces. As we see in Figure 1, the magnetic field of the solar system leads to an increase of mean semi-major axis a in time t . This effect supersedes the solar wind and Poynting-Robertson drag that would otherwise lead to a decrease of a . The secular components of these forces in Delaunay variables (Jancart & Lemaître 2001) reduce to:

$$\frac{dL}{dt} = -\gamma \frac{n \left(1 + \frac{3}{2}e^2\right)}{(1 - e^2)^{3/2}}, \quad \frac{dG}{dt} = -\gamma n, \quad \frac{dH}{dt} = -\gamma n \cos i, \quad (20)$$

while the averaged effect of the drag forces on the angular variables l, g, h turns out to vanish. We notice, that the common proportionality factor γ , different from the definition of Jancart & Lemaître (2001), is simply given by:

$$\gamma = \frac{\beta\mu}{c} \left(1 + \frac{\eta}{Q}\right). \quad (21)$$

By making use of Equation (16) we are able to express Equation (20) in terms of $da/dt, de/dt, di/dt$, respectively. In this section, we focus on solutions where the inward drift in the semi-major axis due to Poynting-Robertson and solar wind drag is balanced with the outward drift due to Lorentz-force. This is the case if the first of Equation (13) equals to $-da/dt$ stemming from the first of Equation (20). By proper arrangement of terms we obtain the condition:

$$\frac{q}{m} = \frac{\beta}{c} \frac{(Q + \eta)}{Q} \frac{n^3 a^{\kappa+2} G_{\kappa}(e)}{r_0^{\kappa} \cos(i)} (B'_N u_{sw} \omega_3)^{-1}, \quad (22)$$

where the functions $G_{\kappa} = G_{\kappa}(e)$ are given in Appendix A. We notice that the above relation is the condition on the physical parameters q/m , β , Q of a micrometer-sized dust particle to be secularly stable for the mean of the orbital elements n , a , e , and i , in a solar wind and magnetic field environment parametrized by η , B'_N , u_{sw} , and ω_3 . Let us denote the surface potential U associated to Equation (22) by the equilibrium surface potential from now on.

2.6. Additional gravitational perturbations

In the previous sections we have disregarded the influence of the planets by setting $m_1 = 0$. This assumption can only be true in regimes of motion within our solar system, where dust grains are not in mean motion resonance with the other planets. For a discussion of the role of such planetary mean motion resonances see Weidenschilling & Jackson (1993); Sicardy et al. (1993); Dermott et al. (1994); Beauge & Ferraz-Mello (1994) or Liou & Zook (1997); Kocifaj & Klačka (2008); Pástor et al. (2009); Lhotka & Celletti (2015). We can expect a quite different dynamical picture for charged dust grains in a resonant lock with the planets as compared to the purely dissipative case. The time of temporary capture and the locations of the resonant regimes of motion in the solar system will be strongly affected by the actual charge of the dust grains, and moreover, by the actual interplanetary magnetic field. This topic deserves further investigations, but is beyond the scope of this study.

3. Numerical simulations & parameter study

We aim in this Section, first, to confirm our analytical results by means of direct numerical integration of Equation (2), and second, we aim to investigate the long term dynamics of dust particles with different exponents κ that determine B_N in Equation (8). We study parameters and initial conditions that are close to the balanced solutions of Equation (2), in particular those solutions that remain close to their initial values on secular times. Furthermore, we perform a parameter study valid for secularly stable, electrically charged dust grains.

In Section 2 we used Equation (2) with B_N given by Equation (8) and b_N taken from Equation (15) with $\kappa = 2$. Here, we use $\kappa = 1, 2, 3$ together with the physical parameters that we summarize in Table 3. Astronomical and physical constants are taken from Luzum et al. (2011); Stöecker (2014). Ranges for various parameters are derived on the basis of proposed values in literature: Burns et al. (1979); Gustafson (1994); Grün et al. (1994), and Kocifaj et al. (2006). Typical optical properties and densities, that are consistent with observations yield $\beta \simeq 0.2/R$ with R given in [μm] (Beauge & Ferraz-Mello 1994), and $\beta \simeq 7.6 \times 10^{-4} A/m$ with A/m given in [m^2/kg] (Kocifaj et al. 2006).

In Figure 2 we show typical orbits close to a secular equilibrium. We set $\kappa = 1$, $U = 5V$, $Q = 1$, $\rho = 2g/cm^3$, and $a(0) = 1au$, $e(0) = 0.1$, $i(0) = 12^\circ$, together with initial angles set to $\omega(0) = \Omega(0) = M(0) = 180^\circ$. From Equation (22) we find $q/m \simeq 2.1 \times 10^{-5}$ that corresponds to $R \simeq 55.5\mu m$ and $\beta \simeq 0.005$. For this values we find a secularly stable orbit on time scales longer than several solar cycles. This solution therefore stays close to its initial semi-major axis, as expected. A higher charge leads to a positive drift, a lower charge to a negative drift in the semi-major axis. For

#	<i>value</i>	<i>unit</i>	<i>ref.</i>
β	$0 \dots 0.5$	–	Gustafson (1994)
q/m	$-0.5 \dots 0.5$	Ckg^{-1}	v.i.
Q	$1 \dots 2$	–	Kocifaj et al. (2006)
R	$0.5 \dots 10$	μm	Grün et al. (1994)
ρ	$0.5 \dots 2$	gcm^{-3}	Grün et al. (1994)
U	$-10 \dots 10$	V	Grün et al. (1994)
B_{R0}, B_{T0}	3.0×10^{-9}	T	Kocifaj et al. (2006)
B_{N0}	0.5×10^{-9}	T	v.i.
c	299792458	kms^{-1}	Luzum et al. (2011)
ε_0	8.854187×10^{-12}	F/m	Stöecker (2014)
Gm_1	1.266865×10^{17}	m^3s^{-2}	Luzum et al. (2011)
η	$1/3$	–	Kocifaj et al. (2006)
μ	1.327124×10^{20}	m^3s^{-2}	Luzum et al. (2011)
S (1au)	1.3608	kW/m^2	Burns et al. (1979)
u_{sw}	400	kms^{-1}	Grün et al. (1994)
$(\omega_1, \omega_2, \omega_3)$	(0.035, 0.121, 0.992)	–	v.i.

Table 1: Physical parameters. The charge is obtained from $q = 4\pi\varepsilon_0UR$, mass from $m = 4/3\pi\rho R^3$, cross section from $A = \pi R^2$. Normal component B_{N0} estimated from $B_{N0} = |B_{R0}|\sin\delta_B$ with meridional angle $\delta_B \simeq 10^\circ$ (Forsyth et al. 2002). The direction of the magnetic z -axis with respect to the inertial plane is given by $\omega_1 = \cos\varnothing \sin\iota$, $\omega_2 = \sin\varnothing \sin\iota$, $\omega_3 = \cos\iota$ with $\varnothing = 73.67^\circ$ and $\iota = 7.25^\circ$, taken from Epstein (1917).

completeness, we also show time series of the remaining orbital elements: the period of the mean anomaly M is nearly constant as we can see in the top-right panel of Figure 2. The eccentricity e of the orbit oscillates around a mean value close to its initial condition, that is only slightly affected by changing q/m , while the argument of perihelion ω rotates. The inclination i of the charged particle stays nearly constant. Finally, the longitude of the ascending node oscillates around its initial condition with very similar amplitudes for different q/m ratios. We like to point out that the essential orbital dynamics is reproduced in all three dynamical models. However, the drift in inclination is overestimated in the purely secular model as one can see in the lower-left panel of Figure 2.

If we repeat our study for $\kappa = 2, 3$ we find the same kind of dynamical behaviour of the particles close to the balanced solutions, see Figure 3: for q/m that leads to secularly stable motions the drift in semi-major axis remains close to zero. For larger deviations ($\pm 500V$) from the value q/m obtained from Equation (22) corresponding to $5V$ the situation changes as follows: for the lower value of q/m the negative drift in semi-major axis a becomes stronger for increasing κ . For larger values of q/m the positive drift becomes weaker. The other orbital elements are only slightly perturbed for increasing κ , while keeping the structural form of the solution (not shown here).

We also perform a parameter study in R , ρ , and Q to check for the dependency of the surface potential U that leads to secularly stable motions, on some typical properties of micro-meter sized dust grains. In Figure 4 we show how the equilibrium voltage for a dust grain located at $1au$ mainly depends on the radius R of the grain. It depends to about 10 – 15% on the quality factor Q , while a dependency on the density ρ would not be visible. We find that U also depends on the exponent κ , i.e. the parametrization of

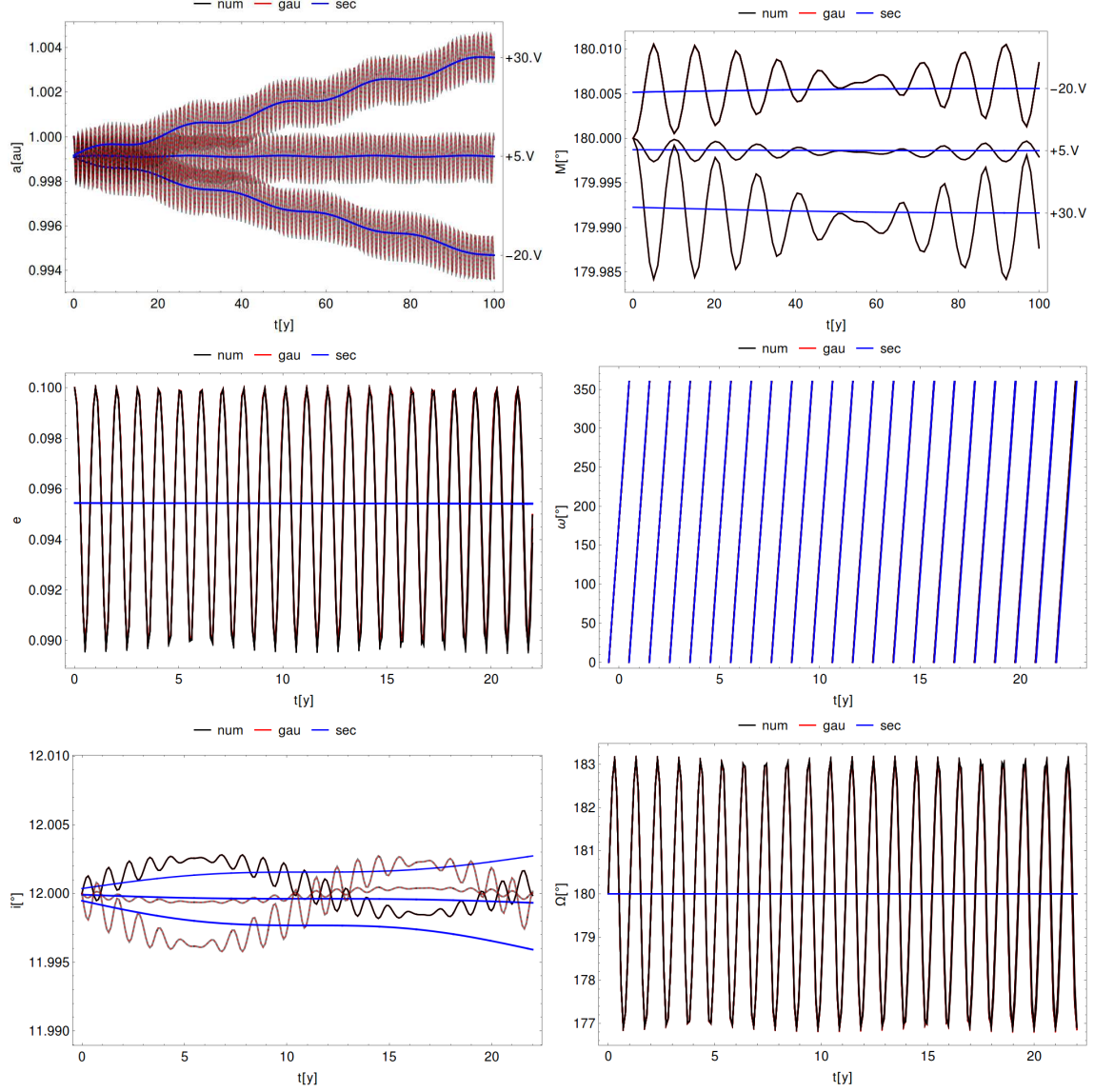


Fig. 2.— Orbital dynamics of charged dust grains in the vicinity of the equilibrium surface potential (5V). Numerical solutions based on Equation (2) (black, *num*), Equation (5) (red, *gau*), and Equations (13), (14) (blue, *sec*), respectively. Small frame ticks on the right indicate surface potential in Volts.

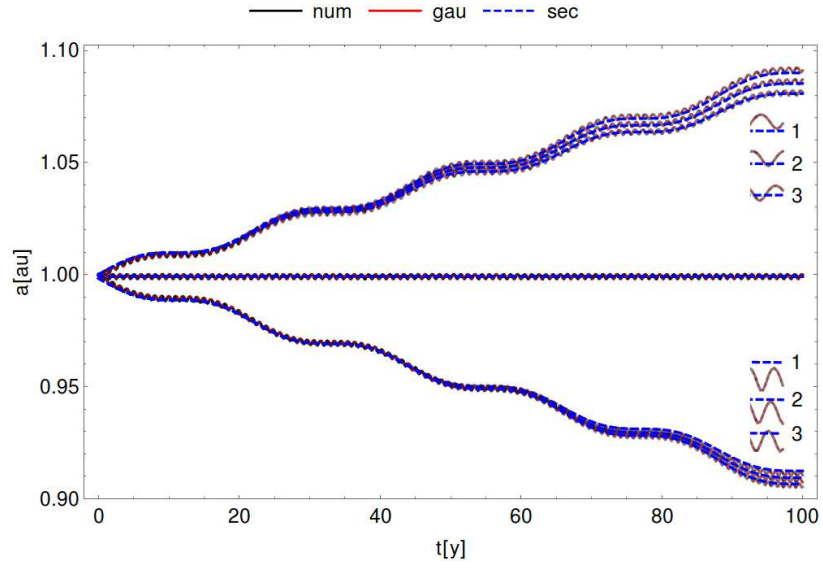


Fig. 3.— Orbital dynamics of charged dust grains in the vicinity of the equilibrium surface potential (5V). Numerical solutions based on Equation (2) (black, *num*), Equation (5) (red, *gau*), and Equations (13), (14) (blue, *sec*), respectively. Ticks inside the figure indicate κ in Equation (8).

the interplanetary magnetic field. We also perform a second parameter study in varying distance a from the Sun for fixed dust particle characteristics. In Figure 5 we clearly see the strong dependency of the equilibrium surface potential U on the interplanetary magnetic field model, i.e. the radial dependence parametrized by the exponent κ .

4. Summary & Conclusions

The orbital stability of charged dust grains in our solar system is strongly affected by various non-gravitational forces, i.e. by the solar wind and the Poynting-Robertson drag forces, as well as the Lorentz force from the interplanetary magnetic field. We therefore investigate the combination of these effects and their influence on the long term dynamics of charged dust grains. Major discoveries from our study on the role of the magnetic field in the micrometer-sized particle dynamics are:

1. The normal component of the magnetic field strongly affects the long-term stability of charged dust particles, leading to secular positive or negative drift in the semi-major axis depending on the actual charge over mass ratio. The normal component of the magnetic field is usually not included in standard models of the interplanetary magnetic field (Parker 1958; Weber & Davis 1967). More realistic magnetic field models that include a normal component will improve our understanding of long-term dust dynamics.
2. There are special values of charge over mass ratios that balances out the solar wind and Poynting-Robertson drag forces with the Lorentz force at given distance from the Sun. This q/m ratios lead to secularly stable motions, and depend on the amplitude of the normal component of the interplanetary magnetic field, the orbital shapes, and the physical properties of the charged particles. The measurement of electric

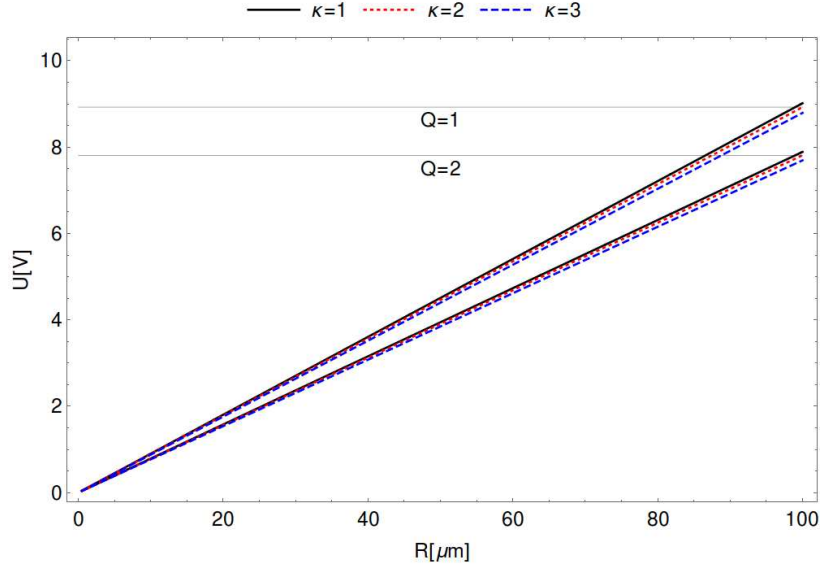


Fig. 4.— Equilibrium surface potential U (in Volts) of charged dust grains at $1au$ for different radii R (in μm) and κ .

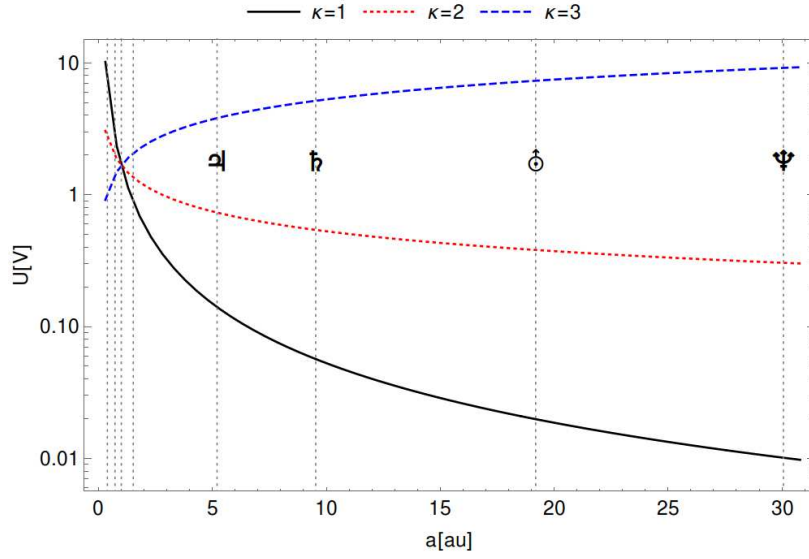


Fig. 5.— Parameter study of the equilibrium surface potential U (in Volts) of charged dust grains with fixed radius $R = 100\mu m$ for different exponents κ in Equation (8). Dotted lines indicate the semi-major axes of the planets.

charge of dust grains during future interplanetary space missions will allow to test our predictions of secularly stable particle orbits for specific q/m ratios.

Moreover, we provide a qualitative description of the dynamics of charged dust grains on the basis of averaging theory: the secular drift in the semi-major axis of charged dust grains turns out to be proportional to the strength of the normal component of the interplanetary magnetic field, the mean solar wind speed, and proportional to the inverse arbitrary exponent κ applied to the distance from the Sun. The direction of the drift (outwards or inwards from the initial distance) strongly depends on the value and sign of the charge over mass ratio. The secular evolution in orbital eccentricity e , and inclination i is of the order of $1/a$ times the drift in the semi-major axis. The drift in a and e turns out to be more effective for smaller inclinations i . On the contrary, the drift in inclination i itself becomes less effective in smaller i . The ratio q/m , that yields secularly stable motions, is proportional to β that depends on the radius, the density, and optical properties of the dust grain. It increases along with the distance from the Sun for $\kappa = 3$ and decreases with $\kappa = 1, 2$. The charge over mass ratio q/m that leads to secularly stable motions turns out to be slightly larger for smaller efficiency factors Q and smaller κ . If these kinds of charged dust grains exist in large amounts then the interplanetary medium may contain a significant amount of charged particles of same parity because there is an asymmetry in the balance of forces: solar wind and Poynting-Robertson drag can only add negative da/dt , while Lorentz force can contribute with $\pm da/dt$. However, only positively charged dust grains may counteract the negative drift if the average of B_N is positive (and vice versa). Therefore, one can expect a larger amount of charged particles of same parity if the mean of the normal field component is non-zero.

Our study is the first of a series of studies on the interplay of the interplanetary magnetic field and charged dust grains within the solar system. We still neglect the

gravitational influence of the major bodies and use a simplified model of the interplanetary magnetic field (i.e. we omit interplanetary magnetic sectors of opposite polarity, and local perturbations of the magnetic field). In addition, applying the assumptions of a radial magnetic field leads to an impossible magnetic monopole in the center of a Parker spiral. However, we would like to stress that Equation (22) holds true for more generic normal magnetic field components B_N . It would therefore be very interesting to clarify if a non-zero average component of the interplanetary magnetic field (or z-component of the solar magnetic axis) exists, at least for sufficient long enough periods of time to trigger secular motions in the orbital dynamics of electrically charged dust grains.

Typical applications of our work are: the dust environment of the solar system in general, i.e. dust that is released by asteroid collisions or by means of cometary activity. The dust environment in the vicinity of the moons and the planets, in particular the Lagrange points of the system. Dust experiments have become part of important interplanetary space missions: the Ulysses spacecraft that was the first to study the Sun from pole to pole. The space probe measurements include the solar wind, charged particles, neutral gases and small particles from the local interstellar space. The Galileo dust detector on board of the Galileo spacecraft was intended to measure dust grains over a wide range of masses in interplanetary space and in the Jovian system. Measurements provide physical and dynamical properties as functions of the distances to the Sun, to Jupiter, and the Jovian satellites. The cosmic dust analyzer on board of the Cassini spacecraft measured the chemical composition of dust during its cruise to Saturn, investigated the Io dust streams during its Jupiter flyby, mapped the size distribution of ring material, and analyzed gravitationally bound ejecta particles in the vicinity of the icy satellites. Future space probes should be able to measure: the dust kinematics (velocity vectors), the dust properties (size, weight, density, optical properties, temperature, chemical composition, and charge), as well as the normal component of the magnetic field environment. The measurements will not only provide important new

insights into the structure of the interplanetary magnetic field, it will also allow to study the physical properties of dust grains that may have strong implications on coagulation and planet formation. Last but not least, it will allow to test the hypothesis of an electrically charged solar system, in terms of secularly stable, electrically charged dust particle orbits.

Appendix A

The secular system defined by Equations (13), (14) comprises the eccentricity functions $g_{\kappa,j}$, valid up to $O(e^5)$, that are given in Table 2. The eccentricity functions $G_{\kappa}(e)$ in Equation (22) for $\kappa \in \{1, 2, 3\}$, expanded up to $O(e^5)$ are:

$$\begin{aligned} G_1(e) &= 1 + 3e^2 + 33e^4/8, \\ G_2(e) &= 1 + 2e^2 + 9e^4/8, \\ G_3(e) &= 1 + e^2/2 - 9e^4/8. \end{aligned} \tag{23}$$

A Taylor series expansion in e of the right hand sides of Equation (5), i.e. $c_{\mathbf{k}}$, $s_{\mathbf{k}}$, may be obtained by one of the authors.

Acknowledgements

We thank M. Bentley for providing material on measurements of physical dust properties. We also thank an anonymous reviewer who greatly helped us to improve a previous version of the manuscript.

κ	1	2	3
$g_{\kappa,a}$	2	$2 + 2e^2 + 2e^4$	$2 + 5e^2 + 8e^4$
$g_{\kappa,e}$	$-e/2 + e^3/8$	$e/2 + e^3/8$	$3e/2 + 3e^3/2$
$g_{\kappa,i}$	$-1/2 - e^2/4 - 3e^4/16$	$-1/2 - e^2/4 - 3e^4/16$	$-1/2 - e^2/2 - e^4/2$
$g_{\kappa,\omega}$	$-1/2$	$-1 - 5e^2/8$	$-3/2 - 9e^2/4$
$g_{\kappa,\Omega}$	$-1/2$	$-1/2 - e^2/4 - 3e^4/16$	$-1/2 - 3e^2/4 - 15e^4/16$
$g_{\kappa,a}$	$-1 + e^2/2$	$-1/2 + e^2/8$	0

Table 2: Eccentricity functions $g_{\kappa,j}$ with $j \in \{a, e, i, \omega, \Omega, M\}$ for $\kappa = 1, 2, 3$, respectively.

REFERENCES

- Beauge, C., & Ferraz-Mello, S. 1994, *Icarus*, 110, 239
- Burns, J. A., Lamy, P. L., & Soter, S. 1979, *Icarus*, 40, 1
- Celletti, A., & Lhotka, C. 2012, *Regular and Chaotic Dynamics*, 17, 273
- Consolmagno, G. J. 1979, *Icarus*, 38, 398
- Dermott, S. F., Jayaraman, S., Xu, Y. L., Gustafson, B. Å. S., & Liou, J. C. 1994, *Nature*, 369, 719
- Dvorak, R., & Lhotka, C. 2013, *Celestial Dynamics: Chaoticity and Dynamics of Celestial Systems* (Wiley-VCH)
- Epstein, T. 1917, *Astronomische Nachrichten*, 204, 351
- Fahr, H. J., Ripken, H. W., & Lay, G. 1981, *A&A*, 102, 359
- Fahr, H. J., Scherer, K., & Banaszkiewicz, M. 1995, *Planet. Space Sci.*, 43, 301
- Fitzpatrick, P. M. 1970, *Principles of celestial mechanics* (Academic Press, New York)
- Forsyth, R. J., Balogh, A., Horbury, T. S., et al. 1996, *Astronomy & Astrophysics*, 316, 287
- Forsyth, R. J., Balogh, A., & Smith, E. J. 2002, *Journal of Geophysical Research (Space Physics)*, 107, 1405
- Grün, E., Gustafson, B., Mann, I., et al. 1994, *A&A*, 286, 915
- Gustafson, B. A. S. 1994, *Annual Review of Earth and Planetary Sciences*, 22, 553
- Hiltula, T., & Mursula, K. 2006, *Geophysical Research Letters*, 33, L03105
- Jancart, S., & Lemaître, A. 2001, *Celestial Mechanics and Dynamical Astronomy*, 81, 75

- Klačka, J. 2013, MNRAS, 436, 2785
- Kocifaj, M., & Klačka, J. 2004, Planet. Space Sci., 52, 839
- . 2008, A&A, 483, 311
- Kocifaj, M., Klačka, J., & Horvath, H. 2006, MNRAS, 370, 1876
- Krivov, A., Kimura, H., & Mann, I. 1998a, Icarus, 134, 311
- Krivov, A., Mann, I., & Kimura, H. 1998b, Earth, Planets, and Space, 50, 551
- Lhotka, C., & Celletti, A. 2013, International Journal of Bifurcation and Chaos, 23, 50036
- . 2015, Icarus, 250, 249
- Liou, J.-C., & Zook, H. A. 1997, Icarus, 128, 354
- Luzum, B., Capitaine, N., Fienga, A., et al. 2011, Celestial Mechanics and Dynamical Astronomy, 110, 293
- Mann, I., Köhler, M., Kimura, H., Cechowski, A., & Minato, T. 2006, A&A Rev., 13, 159
- Mann, I., Meyer-Vernet, N., & Czechowski, A. 2014, Phys. Rep., 536, 1
- Mann, I., Murad, E., & Czechowski, A. 2007, Planet. Space Sci., 55, 1000
- Meyer-Vernet, N. 2007, Basics of the Solar Wind, Cambridge Atmospheric and Space Science Series (Cambridge University Press)
- Morfill, G. E., & Grün, E. 1979a, PSS, 27, 1283
- . 1979b, PSS, 27, 1269
- Mukai, T., & Giese, R. H. 1984, A&A, 131, 355

- Mursula, K., & Virtanen, I. I. 2012, *Journal of Geophysical Research*, 117, A08104
- Parker, E. N. 1958, *ApJ*, 128, 664
- Pástor, P., Klačka, J., & Kómar, L. 2009, *Celestial Mechanics and Dynamical Astronomy*, 103, 343
- Ragot, B. R., & Kahler, S. W. 2003, *ApJ*, 594, 1049
- Sicardy, B., Beauge, C., Ferraz-Mello, S., Lazzaro, D., & Roques, F. 1993, *Celestial Mechanics and Dynamical Astronomy*, 57, 373
- Stöecker, H. 2014, *Taschenbuch der Physik* (Edition Hari Deutsch)
- Wallis, M. K., & Hassan, M. H. A. 1985, *A&A*, 151, 435
- Weber, E. J., & Davis, Jr., L. 1967, *ApJ*, 148, 217
- Weidenschilling, S. J., & Jackson, A. A. 1993, *Icarus*, 104, 244
- Zurbuchen, T. H., Schwadron, N. A., & Fisk, L. A. 1997, *J. Geo. Res.*, 102, 24175